

3-13-2017

# THz Metamaterial Characterization Using THz-TDS

Christopher H. Kodama  
*Air Force Institute of Technology*

Ronald A. Coutu Jr.  
*Marquette University, ronald.coutu@marquette.edu*

---

Published version. "THz Metamaterial Characterization Using THz-TDS," in *Terahertz Spectroscopy* edited by Jamal Uddin. London: IntechOpen, 2017. DOI. © 2017 The Author(s). Licensee InTech. This chapter is distributed under the terms of the Creative Commons Attribution License (<http://creativecommons.org/licenses/by/3.0>), which permits unrestricted use, distribution, and reproduction in any medium, provided the original work is properly cited.

Marquette University

e-Publications@Marquette

***Electrical and Computer Engineering Faculty Research and Publications/College of Engineering***

***This paper is NOT THE PUBLISHED VERSION; but the author’s final, peer-reviewed manuscript.***

The published version may be accessed by following the link in the citation below.

*Terahertz Spectroscopy*, (2017). [DOI](#). This article is © 2017 The Author(s). Licensee InTech and permission has been granted for this version to appear in [e-Publications@Marquette](#). This chapter is distributed under the terms of the Creative Commons Attribution License (<http://creativecommons.org/licenses/by/3.0>), which permits unrestricted use, distribution, and reproduction in any medium, provided the original work is properly cited.

Contents

Abstract.....	2
Keywords.....	2
1. Introduction to metamaterials.....	2
2. Metamaterials analysis and measurement.....	3
3. Fabrication processes.....	5
4. Active metamaterials .....	7
5. Conclusion.....	11
Acknowledgments.....	12
References .....	12

# THz Metamaterial Characterization Using THz-TDS

Christopher H. Kodama

Ronald A. Coutu, Jr.

Marquette University, Milwaukee, WI

## Abstract

The purpose of this chapter is to familiarize the reader with metamaterials and describe terahertz (THz) spectroscopy within metamaterials research. The introduction provides key background information on metamaterials, describes their history and their unique properties. These properties include negative refraction, backwards phase propagation, and the reversed Doppler Effect. The history and theory of metamaterials are discussed, starting with Veselago's negative index materials work and Pendry's publications on physical realization of metamaterials. The next sections cover measurement and analyses of THz metamaterials. THz Time-domain spectroscopy (THz-TDS) will be the key measurement tool used to describe the THz metamaterial measurement process. Sample transmission data from a metamaterial THz-TDS measurement is analyzed to give a better understanding of the different frequency characteristics of metamaterials. The measurement and analysis sections are followed by a section on the fabrication process of metamaterials. After familiarizing the reader with THz metamaterial measurement and fabrication techniques, the final section will provide a review of various methods by which metamaterials are made active and/or tunable. Several novel concepts were demonstrated in recent years to achieve such metamaterials, including photoconductivity, high electron mobility transistor (HEMT), microelectromechanical systems (MEMS), and phase change material (PCM)-based metamaterial structures.

## Keywords

Terahertz; THz; time domain spectroscopy; TDS; metamaterials

## 1. Introduction to metamaterials

In the field of metamaterials, "meta-atoms" are designed to resonate and respond to stimuli in a similar manner as normal atoms.<sup>1</sup> From a macroscopic perspective, a matrix of meta-atoms can be viewed as a single homogeneous material—a metamaterial—with altered material properties. Meta-atoms designed to have electric and magnetic resonances are the base units of electromagnetic metamaterials. These have altered values of electric permittivity and magnetic permeability, which in turn results in a modified refractive index. Acoustic metamaterials, with altered mechanical material properties such as Poisson's ratio, have also been demonstrated.<sup>2</sup> In order to rightfully be considered a homogenous material, the meta-atoms constituting the metamaterial must be sufficiently small. For electromagnetic metamaterials, the meta-atoms need to be at least an order of magnitude smaller than the wavelengths of the desired operating frequencies.<sup>1</sup>

Metamaterials are appealing because they offer the ability to artificially create custom material characteristics without having to depend on the fixed characteristics of existing materials. These metamaterials can further be designed to have exotic properties that are not seen in any naturally existing material. V.G. Veselago, in a paper in 1968, first considered and described the physical

properties that would result from a material with simultaneously negative values of permittivity and permeability. Such materials are known as left-handed media.<sup>1</sup>

In left-handed media, electromagnetic waves have a negative phase velocity; the waves seemingly follow the left-handed rule instead of the normal right-handed one. In addition, negative refraction occurs on a boundary between an ordinary and a left-handed medium. Negative refraction also causes left-handed concave and convex lenses to have reversed behavior: the concave lens converges light, and the convex lens diverges it. Surprisingly, a flat slab of left-handed material can even be used as a focusing lens.<sup>3</sup> Other exotic effects include inverse versions of the Doppler effect, Cerenkov radiation (i.e., radiative shock waves induced by high-speed particles traveling through a dielectric medium), and the Goos-Hänchen shift (i.e., a finite lateral shift between an incident beam of finite extent and its reflected counterpart).<sup>1</sup>

Although Veselago had established theoretical groundwork for understanding the nature negative-index materials, experimental demonstration of these materials would not occur for a few decades.<sup>3,4</sup>

J.B. Pendry in the late 1990s was the first to examine the fabrication of materials with customizable permeabilities and permittivities. In 1998, he demonstrated that a thin wire mesh would excite low frequency plasmons, meaning that the mesh would have customized, effective homogeneous permittivity values at low frequencies; these values could even be negative.<sup>4</sup> Soon after, he proposed a split-ring resonator (SRR) structure, which could analogously produce a desired effective permeability (including negative values) in the GHz range.<sup>5</sup> The structures he proposed, especially the split-ring resonator structure, are now ubiquitous in metamaterial devices at all frequencies.

The unique properties of metamaterials make them prime targets for research in the RF and photonics fields, where metamaterials can be used for enhanced lensing, beam steering, and phase shifting. Metamaterials have also greatly advanced the field of cloaking by freeing up the restriction of only being able to use naturally occurring materials and their material properties. Several different cloaking techniques have been demonstrated using metamaterials.<sup>6-9</sup>

The THz spectrum has much potential for future applications, ranging from communications to bomb screening. Unfortunately, since most materials are transparent in the THz frequency range, controlling THz waves via modulation and other techniques is much more difficult when compared to electronic or optical devices and systems; metamaterials can help fill this technology gap. Since metamaterials can, in theory, be specifically designed to have certain material properties, they can interact with THz waves in ways that normal materials cannot.<sup>10,11</sup>

## 2. Metamaterials analysis and measurement

The split-ring resonator (SRR) is the fundamental unit cell used in a multitude of metamaterial designs. SRRs are split metallic rings meant to resonate with electromagnetic waves with wavelengths much larger than the SRR structure itself. The first SRRs proposed by Pendry consisted of two circular, concentric rings with oppositely oriented splits, as shown in [Figure 1\(a\)](#). For the sake ease of fabrication, SRRs fabricated in the THz range typically have a much simpler geometry, like shown in [Figure 1\(b\)](#).

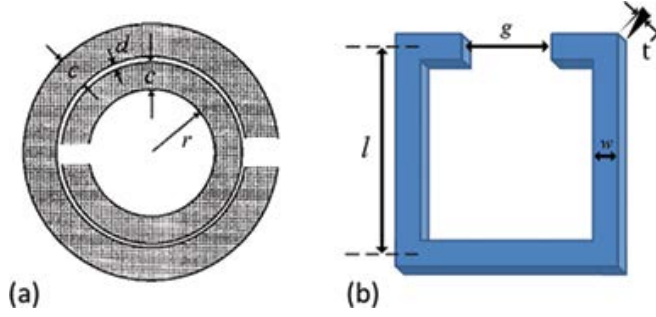


**Figure 1.** (a) Original SRR proposed by Pendry [5]; (b) a typical SRR shape used in THz research.<sup>11,12</sup>

SRRs are not the only method of generating resonant responses. In theory, pieces of metal in any geometrical shape can act as a resonator, albeit at frequencies determined by the geometry. For example, simple structures like rectangular hole arrays support surface wave polariton (SPP) resonant modes that can also strongly enhance incident radiation.<sup>13</sup> However, SRRs have two characteristics that make them desirable for use in metamaterials. SRRs couple well with the magnetic portion of electromagnetic waves due to its loop-like structure. This potentially allows SRR-containing metamaterials to have a frequency band with negative permeability. Second, the SRR is easily conceptualized as a simple LC resonator circuit, which allows one to quickly predict its lowest order resonant frequency.

As a basic approximation, the entire loop (ignoring the gap) can be viewed as a one-turn inductor and the gap as a parallel-plate capacitor. These quasi-static assumptions require that the dimensions of the SRR be much smaller than the wavelength of electromagnetic fields assumed to be passing through them (which conveniently is the same requirement needed to produce effective material properties from metamaterials). The wavelength of electromagnetic waves in free space at 1 THz is 300  $\mu\text{m}$ , so metamaterial unit cells designed to operate in this range should have maximum dimensions of around 30  $\mu\text{m}$  or less. The basic equations for the inductance, capacitance, and estimated resonant frequency of an SRR are

$$L \approx \mu_0 \frac{t^2}{t}, C \approx \epsilon_r \epsilon_0 \frac{tw}{g}, f_{ideal} \approx \frac{1}{2\pi} \sqrt{\frac{1}{LC}} = \frac{1}{2\pi} \frac{c}{\sqrt{\epsilon_r}} \sqrt{\frac{g}{wl^2}}, \text{E1}$$

where  $t$  is the thickness of the SRRs,  $\mu_0$  is the vacuum permeability constant,  $l$  is the SRR side length,  $\epsilon_r$  is the relative dielectric constant,  $\epsilon_0$  is the vacuum permittivity constant,  $w$  is the line width of the SRR,  $g$  is the gap width of the SRR, and  $c$  is the speed of light in vacuum.<sup>14-16</sup>

The lowest order resonance of a SRR can be adequately described by a quasistatic model incorporating capacitors and resistors. The higher order resonances, however, cannot be modeled in such a manner. The original SRR in [Figure 1\(a\)](#) can be modeled as a transmission line due to the presence of two distinct conductors.<sup>17</sup> The single SRR in [Figure 1\(b\)](#) has only one conductor and thus cannot support any transmission line modes. Single SRRs can, however, produce evanescent modes confined to the surface, known as plasmon resonances. These plasmonic resonances occur at frequencies that have half-wavelengths, which are multiples  $m$  of the perimeter of the SRR:

$$f_{dip} = \frac{c}{\sqrt{\epsilon_{r,eff}}} \frac{1}{(4l-g)} \frac{m}{2}, \text{E2}$$

where  $c$  is the speed of light,  $\epsilon_{r,eff}$  is the effective permittivity constant,  $l$  is the side length of the square SRR,  $g$  is the gap length of the SRR, and  $m$  is a positive integer greater than or equal to 1.<sup>1</sup> The LC resonance can also be interpreted as the lowest order plasmon resonance, with  $m = 1$  in the above equation.<sup>18</sup>

These equations can only serve as basic approximations for the resonant frequency of a fabricated SRR. This is especially true in the THz range, where limits on feature size lead to non-idealities such as significant wire widths and gap widths. If more accuracy is desired, more precise equations need to be utilized for the inductance and capacitance terms for the LC resonant frequency, and the effective SRR perimeter seen by higher order resonances will differ from simply  $(4l - g)$ , depending on the current distribution through the width of SRR. As an alternative to an analytical solution, SRRs can instead be modeled using electromagnetic simulation software such as CST Microwave Studio, ANSYS HFSS, or COMSOL.

Fabricated THz SRRs can be measured and characterized using THz time-domain spectroscopy (THz-TDS). In THz-TDS, broadband THz pulses are passed through a sample and then are Fourier transformed to obtain spectral data. A simple planar SRR structure is shown in Figure 2(a). The SRR is patterned in a layer of gold, atop an intrinsic silicon substrate; the alignment of the incident THz pulse is shown in the inset. The solid line in Figure 2(b) represents the transmission coefficient of the THz pulse passed through the sample. The LC resonance can be seen at approximately 0.8 THz, and a higher order resonance can be seen near 2.2 THz. The dashed orange line represents simulated data from models in CST Microwave Studio. The simulated data agree well with measured data, except in the region near 2.5 THz and above. In this region, the spectral power in the measured signal is not strong enough to fully resolve the sharp, higher order resonances of the SRR.<sup>19</sup>

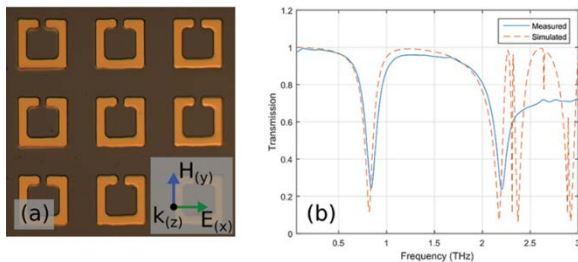


**Figure 2.** Gold SRRs on silicon substrate are shown in (a). The SRRs are 20- $\mu\text{m}$  squares with 5- $\mu\text{m}$  line widths, 3- $\mu\text{m}$  gap widths, and a 39- $\mu\text{m}$  periodicity. The plot in (b) displays the transmission response of the SRRs.<sup>19</sup>

### 3. Fabrication processes

Since THz metamaterial unit cells need to be electrically small compared to THz wavelengths, these unit cells have widths of around 30  $\mu\text{m}$  or less. This requirement makes microfabrication and micro-electromechanical systems (MEMS) processes suitable choices for creating THz metamaterials.

There are three main techniques that can be used to make microelectronic and MEMS devices: bulk micromachining, surface micromachining, and microforming. These techniques are often used interchangeably to create complete devices. In all three of these techniques, the process of photolithography plays an important part in creating devices out of designs.

In photolithography, a layer of photoresist—a polymer sensitive to certain wavelengths of light, typically in the ultraviolet range—is selectively exposed to light screened by a patterned mask. The exposed sections of photoresist undergo a chemical change, depending on the type of polymer. For “positive” photoresist, the exposed photoresist weakens and will dissolve in a developer solution, leaving behind a patterned layer of unexposed photoresist. This patterned photoresist can then act as a mask for other processing steps.

For example, the gold MMs shown in [Figure 2\(a\)](#) could have been fabricated using the process shown in [Figure 3](#) , if a suitably thick photoresist was used along with an evaporation deposition process, which would deposit highly nonconformal material to the edges of the resist. Otherwise, there will be difficulty stripping the photoresist in the fourth step. More advanced, dual-layer photoresist patterning techniques can also be used to create crisper patterns or to be used in conjunction with conformal depositions like sputter deposition. Processes involving the incremental addition and/or etching of thin layers of material on a substrate to create a device are known as surface micromachining techniques.

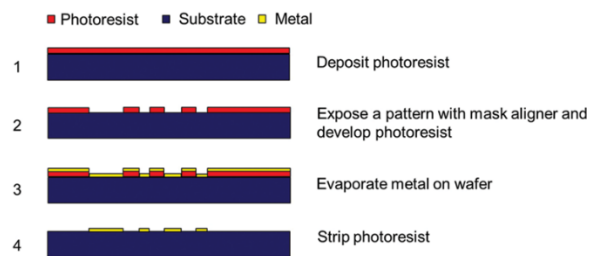


**Figure 3.** An example of the use of photolithography to deposit gold.

In bulk micromachining techniques, a device is fabricated primarily through etching processes into the bulk of a substrate. Depending on the crystallography of the substrate and the etchant type, etching processes can be isotropic or highly anisotropic in certain crystallographic directions. There are also more involved methods, such as deep reactive ion etching (DRIE), which can create high aspect ratio structures through sequential reactive ion etching (RIE) of a sidewall-protected cavity.<sup>20</sup>

Microforming processes, also known as high aspect ratio micromachining (HARM) processes, use especially thick, patterned photoresist layers as molds for metal layers deposited via electroplating. In the LIGA microforming method, X-ray-based photoresist PMMA can be patterned in thick layers without worry of diffraction to create very high aspect ratio devices. LIGA is an acronym for the three German words lithographie, galvanofornung, and abformung, which, respectively, stand for lithography, electroplating, and polymer replication.<sup>21–23</sup> Other thick photoresists such as SU-8, or multiple layers of SF-11, can also be used as a lower cost alternative to create high aspect ratio structures.

In addition to micromachining and MEMS processes, additive manufacturing techniques show promise for THz metamaterials. One advantage to additive manufacturing is the ability to create devices without requiring labor-intensive cleanroom methods. However, the present capability of many of these techniques does not allow for the sub-millimeter resolution needed to create THz metamaterials, with a few exceptions. In inkjet printing, droplets of material are deposited onto a substrate via moving, microscopic nozzle heads. This method has been shown to feasibly fabricate layers of SRRs in the low THz range.<sup>24–26</sup> Inkjet-printed SRRs display resonances that are similar but slightly degraded compared to their cleanroom-fabricated counterparts; the degradation is largely caused by print variation among the

individual printed metamaterial unit cells. This can be seen as a tradeoff to the advantages of less labor-intensive processes and lower cost manufacturing offered by inkjet printing. Another additive manufacturing method used to create THz metamaterials is laser decal transfer.<sup>27</sup> In this process, a laser pulse ejects a small amount of material from a donor substrate and transfers it onto an underlying substrate. The process is analogous to a pen (the laser) writing on top of a piece of carbon paper. Using a digital micromirror device (DMD), the laser can be spatially modulated to transfer more complex shapes onto a target substrate. With this process and an x-y stage manipulator, metal SRRs were printed with a minimum feature size of 6  $\mu\text{m}$ .<sup>28</sup> The printed SRRs were highly uniform and produced a transmission response nearly identical to that of a comparable lithographically prepared sample. The main limitation of this method is that the deposited material needs to be cured at around 150°C after laser transfer, so it may not be suitable for some temperature-sensitive applications.

#### 4. Active metamaterials

Metamaterials with magnetic resonances in the THz range were first demonstrated by Yen et al. in 2004.<sup>29</sup> They were able to couple into the strong magnetic modes of the SRRs by sending incident waves at oblique angles in ellipsometry experiments. There is much ongoing work on developing active THz metamaterials through several methods.<sup>10,30–32</sup> In order for metamaterials to be useful in dynamic applications like modulation, they need an incorporated active component that can modify its resonance.<sup>33</sup>

An active metamaterial was first demonstrated by Padilla et al. in 2006.<sup>34</sup> They successfully shunted the SRR response of single SRRs on a GaAs substrate by utilizing an optical pump. Without any optical excitation, the SRRs exhibited a typical LC resonance. When the optical pump was activated, photo-excited carriers spontaneously formed across the entire surface of the GaAs wafer, which made the entire surface metallic. This in turn nullified the effects of the SRRs and their LC resonance. Nonlinear response can also be achieved through SRRs fabricated on doped GaAs layers.<sup>35</sup> With this technique, incident THz radiation of zero to low levels causes a metallic response due to the doped GaAs layer. However, with increasing THz field strengths, inter-valley scattering becomes more frequent, causing decreased carrier mobility and decreased conductivity. With the disappearance of the suppressing GaAs conductivity, the SRR's LC resonance becomes more prominent, and a notch appears in the transmission. At even higher incident radiation strengths, impact ionization in the gaps of the SRRs causes the conductivity to increase again, suppressing SRR response.

Building on those results, Chen and Padilla demonstrated modulation through voltage-biased SRRs on n-GaAs, with the SRR-nGaAs junction acting as a Schottky barrier.<sup>30,31</sup> This design is shown in [Figure 4](#). Without the presence of a bias voltage, the doped layer effectively suppresses the resonant response. When a high enough voltage is applied between the SRRs and the n-GaAs layers, a depletion region will form underneath the SRRs. This depletion region both electrically isolates the SRRs from the n-GaAs layer and reduces the overall conductivity of the n-GaAs layer, which restores the suppressed LC resonance of the SRRs.



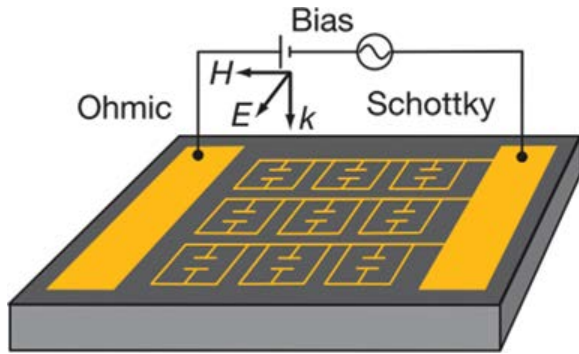


**Figure 4.** Schottky-based modulation of split-ring resonator resonances.<sup>31</sup>

In 2007, Chen et al. demonstrated modulation via frequency shifting by using SRRs enhanced with silicon in the capacitor gaps, as shown in Figure 5.<sup>36</sup> When the SRRs are exposed to laser pulses, photoexcited carriers in the silicon layer effectively lengthen the internal SRR capacitor, which alters the resonant frequency of the structure.

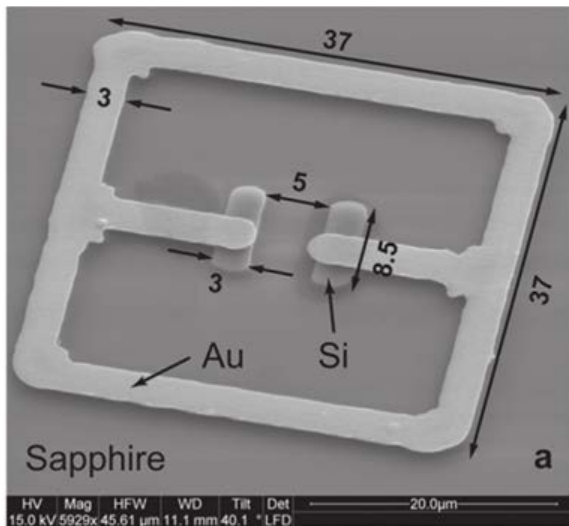


**Figure 5.** Split-ring resonator modulated through photoexcited silicon.<sup>36</sup>

Shrekenhamer and Rout created a novel THz metamaterial design that incorporated high electron mobility transistors (HEMTs) in the gaps of SRRs, as shown in Figure 6.<sup>37</sup> At zero volts gate bias, a 2D electron gas channel naturally forms between the source and drain of the pHEMT, which is connected to opposite sides of the SRR gap. The electron channel shorts the SRR gap and removes the LC resonance from the structure's response. When a negative bias is applied to the gate, the channel is eliminated, and the SRR LC resonance is restored.

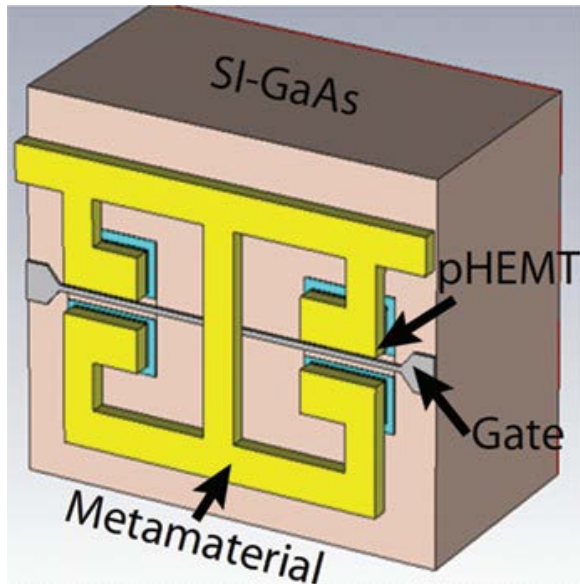


**Figure 6.** High electron mobility transistor–based modulation of split-ring resonators.<sup>37</sup>

The four previously mentioned active metamaterial structures used electrical properties, namely semiconductors and semiconductor junctions, to achieve tunability in the THz frequency range. Mechanically tunable SRRs have also been demonstrated using MEMS processes. For example, Coutu et al. used MEMS cantilever beams arrays to create electrostatically tunable meta-atoms for the RF frequency range.<sup>38</sup> There have since been several demonstrations of THz-range meta-atoms using MEMS. In one such design, bi-material cantilevers are used to alter the resonance of SRRs, shown in Figure 7(a).<sup>39</sup> In the rest state, the cantilevers are bent downward due to residual stresses intentionally introduced during the fabrication process. This shorts the SRR gaps and eliminates the LC resonance. When the device is heated, thermal expansion coefficient difference between the top and bottom half of the cantilever causes the beam to straighten out, which removes the electrical contact and restores the LC resonance. In,<sup>40</sup> the capacitor arms themselves are treated as bi-material cantilevers, which are designed to have an initial deflection and can be lowered with an external voltage. This is shown in Figure 7(b).

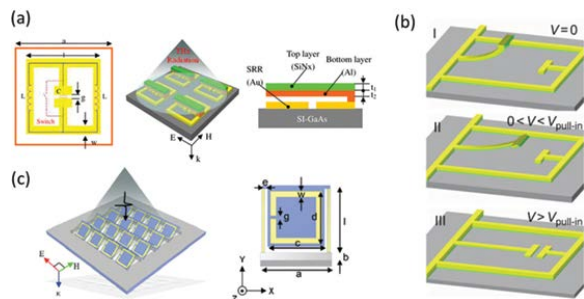


**Figure 7.** Various microelectromechanical systems (MEMS) incorporated, terahertz (THz) frequency range, tunable split-ring resonator (SRR) elements. In (a), THz SRRs are modulated using bi-material cantilevers.<sup>39</sup> The design in (b) uses bi-material cantilevers for the inner capacitive gap arms of THz SRRs, modulating the SRR resonances when these arms are deflected.<sup>40</sup> The third design in (c) shows structurally tunable THz SRRs which use bi-material cantilevers to bend the entire array in different directions.<sup>41</sup>

Bi-material cantilevers can also be used to actively change the in-plane orientation of SRRs, as shown in [Figure 7\(c\)](#).<sup>42</sup> By changing the angle of incidence of the incoming electromagnetic wave with respect to the metamaterial unit cell, the magnetic coupling between the SRRs and the incident wave can be enhanced, strengthening the measured resonance.

Another method of modulating metamaterials is through the use of phase change materials (PCMs) and metal-insulator transition (MIT) materials. PCMs and MIT materials are types of materials that have vastly different electrical and/or optical properties based on their crystallographic alignment.<sup>43,44</sup> Transitions between crystalline and amorphous states can be rapidly achieved, typically through thermal, optical, or electrical methods.

Bouyge et al. demonstrated reconfigurable bandpass filtering by using vanadium dioxide ( $\text{VO}_2$ ) switches on microwave-range SRRs.<sup>45</sup> Vanadium dioxide is a MIT material with a transition temperature of 340 K and is volatile, meaning that it will revert back to its original phase after cooling back down.<sup>44</sup> With the  $\text{VO}_2$  acting as a reconfigurable switch, patches of metal could be electrically connected or disconnected to the SRR, thus altering the resonance of the structure.

Active metamaterial structures designed for the near-infrared range, like the one shown in [Figure 8](#), have also been demonstrated using vanadium dioxide.<sup>46</sup> The planar hybrid structure shown can switch between electrically appearing as a normal SRR surface when the  $\text{VO}_2$  is insulating or a full metal plane when the  $\text{VO}_2$  has transitioned to the conductive state. The  $\text{VO}_2$  in the self-aligned hybrid SRR causes a slight shift in the resonant frequency of the SRR before and after phase transition.

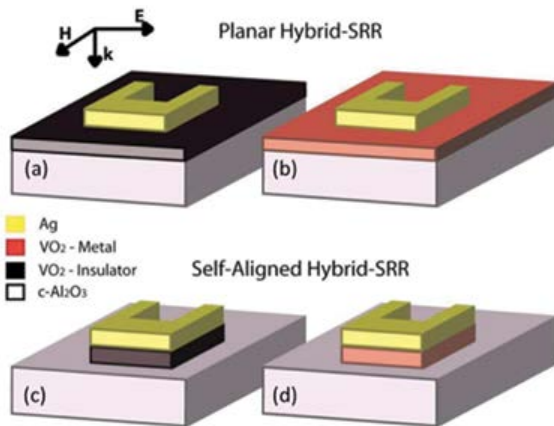


**Figure 8.** Near-infrared metamaterials with vanadium dioxide ( $\text{VO}_2$ ). In (a) and (b), gold split ring resonators (SRRs) are fabricated on a layer of  $\text{VO}_2$ . In (a), before transitioning the  $\text{VO}_2$  layer, the  $\text{VO}_2$  acts like a dielectric and the SRR response is dominates the behavior of the device. In (b), while the  $\text{VO}_2$  layer is transitioned, the  $\text{VO}_2$  layer is metallic and the overall response of the material is that of a flat metal plane. In (c) and (d), the SRRs have two materials in their thickness, a metal layer and a  $\text{VO}_2$  layer. Before transitioning, as shown in (c), the  $\text{VO}_2$  is a dielectric, which only affects the response of the SRR with a small red-shift. In (d), during the  $\text{VO}_2$  transition to a metallic phase, the effective metal thickness of the SRR doubles, which slightly increases the resonant frequency of the device.<sup>46</sup>

Phase change materials have also been applied in some rudimentary metamaterial and plasmonics designs. Phase change materials differ from MIT materials in the fact that their phase transitions are nonvolatile, meaning that an amorphous PCM will crystallize on heating but would not reamorphize on slow cooling. To successfully reamorphize a PCM, a fast heat pulse (from a laser, via Joule heating, etc.)

accompanied by a strong heat sink is needed to “melt-quench” the material back into an amorphous phase. A dynamic metamaterial switch using germanium antimony telluride (GST) is shown in Figure 9.<sup>47</sup> This switch is controlled by a short laser pulse, which can transition the GST between the conductive and insulating states. In addition to GST, the chalcogenide gallium lanthanum sulfide (GLS) has also been shown to have potential for an active, plasmonics-based switch<sup>48</sup> and tunable layer for metamaterials in the infrared range.<sup>49</sup>

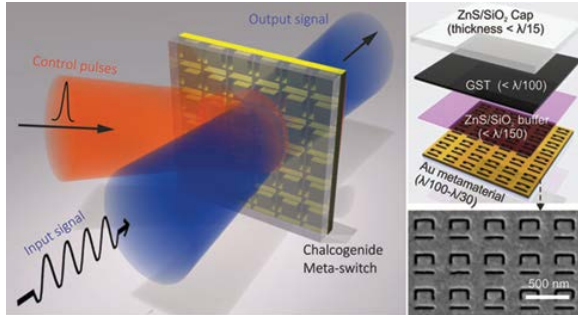


**Figure 9.** Metamaterial absorber with incorporated phase change material layer for dynamic applications.<sup>47</sup>

Kodama et al. have demonstrated the use of germanium telluride (GeTe), another PCM, for achieving tunable SRRs. As shown in Figure 10, GeTe layer was placed in the gaps of SRRs. When the GeTe is amorphous and insulating, the SRRs exhibit their typical LC resonance; when the GeTe is crystalline and conductive, the SRR gap becomes electrically shorted, and the LC resonance is eliminated.

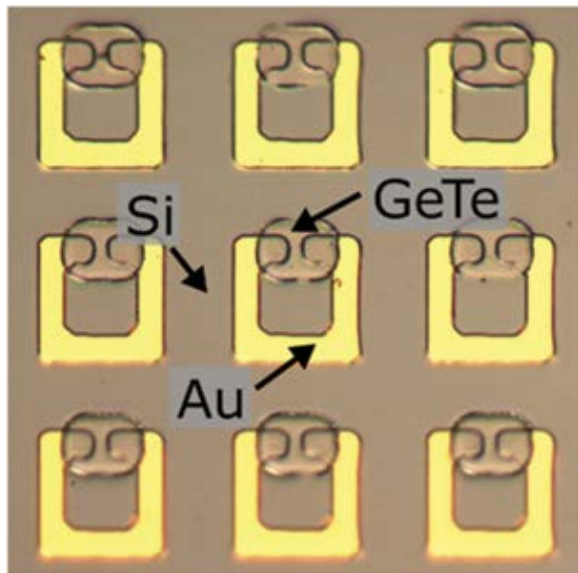


**Figure 10.** Tunable split-ring resonators using germanium telluride in the split gaps.<sup>19</sup>

## 5. Conclusion

This chapter was designed to familiarize the reader with terahertz metamaterials. Starting with fundamental metamaterial unit, cell concepts were outlined, methods for producing metamaterial samples were detailed, and the latest developments in active THz metamaterial research have been

reviewed. We hope we have been able to convey the potential that metamaterial research has to offer for terahertz technologies and systems.

## Acknowledgments

The authors thank the Air Force Office of Scientific Research (AFOSR) for funding this effort (F4FGA06141J001) and the Air Force Research Laboratory (AFRL) Sensors Directorate for their assistance. The authors also thank the Air Force Institute of Technology (AFIT) cleanroom staff, Mr. Richard Johnston and Mr. Adam Fritche.

## References

- [1] R. Marqués, F. Martín, and M. Sorolla, *Metamaterials with Negative Parameters: Theory, Design and Microwave Applications*, 1st ed. Hoboken: Wiley, 2013.
- [2] M.-H. Lu, L. Feng, and Y.-F. Chen, "Phononic crystals and acoustic metamaterials," *Mater. Today*, vol. 12, no. 12, pp. 34–42, Dec. 2009.
- [3] V. G. Veselago, "The electrodynamics of substances with simultaneously negative values of  $\epsilon$  and  $\mu$ ," *Sov. Phys. Uspekhi*, vol. 10, no. 4, p. 509, 1968.
- [4] J. B. Pendry, A. J. Holden, D. J. Robbins, and W. J. Stewart, "Low frequency plasmons in thin-wire structures," *J. Phys. Condens. Matter*, vol. 10, no. 22, p. 4785, 1998.
- [5] J. B. Pendry, A. J. Holden, D. J. Robbins, and W. J. Stewart, "Magnetism from conductors and enhanced nonlinear phenomena," *Microw. Theory Tech. IEEE Trans.*, vol. 47, no. 11, pp. 2075–2084, Nov. 1999.
- [6] S. A. Cummer, B.-I. Popa, D. Schurig, D. R. Smith, and J. Pendry, "Full-wave simulations of electromagnetic cloaking structures," *Phys. Rev. E*, vol. 74, no. 3, p. 36621, Sep. 2006.
- [7] P. Collins and J. McGuirk, "A novel methodology for deriving improved material parameter sets for simplified cylindrical cloaks," *J. Opt. A Pure Appl. Opt.*, vol. 11, no. 1, p. 15104, 2009.
- [8] L. Pei-Ning, L. You-Wen, M. Yun-Ji, and Z. Min-Jun, "A multifrequency cloak with a single shell of negative index metamaterials," *Chin. Phys. Lett.*, vol. 28, no. 6, p. 64206, 2011.
- [9] F. Bilotti, S. Tricarico, and L. Vegni, "Plasmonic metamaterial cloaking at optical frequencies," *Nanotechnol. IEEE Trans.*, vol. 9, no. 1, pp. 55–61, Jan. 2010.
- [10] R. D. Averitt, W. J. Padilla, H. T. Chen, J. F. O'Hara, A. J. Taylor, C. Highstrete, M. Lee, J. M. O. Zide, S. R. Bank, and A. C. Gossard, "Terahertz metamaterial devices," in *Proc. SPIE*, 2007, vol. 6772, p. 677209.
- [11] W. Withayachumnankul and D. Abbott, "Metamaterials in the terahertz regime," *Photonics J. IEEE*, vol. 1, no. 2, pp. 99–118, Aug. 2009.
- [12] C. H. Kodama, *Tunable Terahertz Metamaterials with Germanium Telluride Components*, Air Force Institute of Technology, Dayton, OH, 2016.
- [13] A. K. Azad and W. Zhang, "Resonant terahertz transmission in subwavelength metallic hole arrays of sub-skin-depth thickness," *Opt. Lett.*, vol. 30, no. 21, pp. 2945–2947, Nov. 2005.
- [14] O. Sydoruk, E. Tatartschuk, E. Shamonina, and L. Solymar, "Analytical formulation for the resonant frequency of split rings," *J. Appl. Phys.*, vol. 105, no. 1, p. 014903-1 - 014903-4, 2009.
- [15] J. C. Maxwell, *A Treatise on Electricity and Magnetism*, vol. 1. Dover, Dover Publications, New York, 1954.
- [16] E. B. Rosa and F. W. Grover, "Formulas and tables for the calculation of mutual and selfinductance," *Bull. Bur. Stand.*, vol. 8, pp. 1–287, 1912.

- [17] M. Shamonin, E. Shamonina, V. Kalinin, and L. Solymar, "Resonant frequencies of a split-ring resonator: analytical solutions and numerical simulations," *Microw. Opt. Technol. Lett.*, vol. 44, no. 2, pp. 133–136, 2000
- [19] C. H. Kodama and R. A. Coutru, "Tunable split-ring resonators using germanium telluride," *Appl. Phys. Lett.*, vol. 108, no. 23, 2016.
- [20] F. Laermer and A. Schilp, "Method of Anisotropically Etching Silicon." Google Patents, 1996.
- [21] S. A. Campbell, *Fabrication Engineering at the Micro- and Nanoscale*, 4th ed. New York: Oxford University Press, 2013.
- [22] V. Saile, "Introduction: LIGA and Its Applications," in *LIGA and Its Applications*, Germany: Wiley-VCH Verlag GmbH & Co. KGaA, 2009, pp. 1–10.
- [23] P. Rai-Choudhury, *Handbook of Microlithography, Micromachining, and Microfabrication: Micromachining and Microfabrication*. SPIE Optical Engineering Press, London, UK, 1997.
- [24] K. Takano, T. Kawabata, C.-F. Hsieh, K. Akiyama, F. Miyamaru, Y. Abe, Y. Tokuda, R.-P. Pan, C.-L. Pan, and M. Hangyo, "Fabrication of terahertz planar metamaterials using a super-fine ink-jet printer," *Appl. Phys. Express*, vol. 3, no. 1, p. 16701, 2010.
- [25] H. Teguh Yudistira, A. Pradhipta Tenggara, V. Dat Nguyen, T. Teun Kim, F. Dian Prasetyo, C. Choi, M. Choi, and D. Byun, "Fabrication of terahertz metamaterial with high refractive index using high-resolution electrohydrodynamic jet printing," *Appl. Phys. Lett.*, vol. 103, no. 21, 2013.
- [26] M. Walther, A. Ortner, H. Meier, U. Löffelmann, P. J. Smith, and J. G. Korvink, "Terahertz metamaterials fabricated by inkjet printing," *Appl. Phys. Lett.*, vol. 95, no. 25, 2009.
- [27] R. C. Y. Auyeung, H. Kim, S. Mathews, and A. Piqué, "Laser forward transfer using structured light," *Opt. Express*, vol. 23, no. 1, pp. 422–430, Jan. 2015.
- [28] H. Kim, J. S. Melinger, A. Khachatryan, N. A. Charipar, R. C. Y. Auyeung, and A. Piqué, "Fabrication of terahertz metamaterials by laser printing," *Opt. Lett.*, vol. 35, no. 23, pp. 4039–4041, Dec. 2010.
- [29] T. J. Yen, W. J. Padilla, N. Fang, D. C. Vier, D. R. Smith, J. B. Pendry, D. N. Basov, and X. Zhang, "Terahertz magnetic response from artificial materials," *Science (80-. )*, vol. 303, no. 5663, pp. 1494–1496, 2004.
- [30] K. Fan and W. J. Padilla, "Dynamic electromagnetic metamaterials," *Mater. Today*, vol. 18, no. 1, pp. 39–50, Jan. 2015.
- [31] H.-T. Chen, W. J. Padilla, J. M. O. Zide, A. C. Gossard, A. J. Taylor, and R. D. Averitt, "Active terahertz metamaterial devices," *Nature*, vol. 444, no. 7119, pp. 597–600, Nov. 2006.
- [32] I. B. Vendik, O. G. Vendik, M. A. Odit, D. V. Kholodnyak, S. P. Zubko, M. F. Sitnikova, P. A. Turalchuk, K. N. Zemlyakov, I. V. Munina, D. S. Kozlov, V. M. Turgaliev, A. B. Ustinov, Y. Park, J. Kihm, and C.-W. Lee, "Tunable metamaterials for controlling THz radiation," *Terahertz Sci. Technol. IEEE Trans.*, vol. 2, no. 5, pp. 538–549, Sep. 2012.
- [33] M. Rahm, J.-S. Li, and W. Padilla, "THz wave modulators: a brief review on different modulation techniques," *J. Infrared Millim. Terahertz Waves*, vol. 34, no. 1, pp. 1–27, 2013.
- [34] W. J. Padilla, a. J. Taylor, C. Highstrete, M. Lee, and R. D. Averitt, "Dynamical electric and magnetic metamaterial response at terahertz frequencies," *Phys. Rev. Lett.*, vol. 96, no. 10, p. 107401, Mar. 2006.
- [35] K. Fan, H. Y. Hwang, M. Liu, A. C. Strikwerda, A. Sternbach, J. Zhang, X. Zhao, X. Zhang, K. A. Nelson, and R. D. Averitt, "Nonlinear terahertz metamaterials via field-enhanced carrier dynamics in GaAs," *Phys. Rev. Lett.*, vol. 110, no. 21, p. 217404, May 2013.

- [36] H.-T. Chen, J. F. O'Hara, A. K. Azad, A. J. Taylor, R. D. Averitt, D. B. Shrekenhamer, and W. J. Padilla, "Experimental demonstration of frequency-agile terahertz metamaterials," *Nat Phot.*, vol. 2, no. 5, pp. 295–298, May 2008.
- [37] D. Shrekenhamer, S. Rout, A. C. Strikwerda, C. Bingham, R. D. Averitt, S. Sonkusale, and W. J. Padilla, "High speed terahertz modulation from metamaterials with embedded high electron mobility transistors," *Opt. Express*, vol. 19, no. 10, pp. 9968–9975, May 2011.
- [38] R. A. Coutu, P. J. Collins, E. A. Moore, D. Langley, M. E. Jussaume, and L. A. Starman, "Electrostatically tunable meta-atoms integrated with in situ fabricated MEMS cantilever beam arrays," *Microelectromech. Syst. J.*, vol. 20, no. 6, pp. 1366–1371, Dec. 2011.
- [39] H. Tao, A. Strikwerda, C. Bingham, W. J. Padilla, X. Zhang, and R. D. Averitt, "Dynamical control of terahertz metamaterial resonance response using bimaterial cantilevers," in *Progress in Electromagnetics Research Symposium*, Electromagnetics Academy, 2008, pp. 856–859.
- [40] F. Ma, L. Yu-Sheng, Z. Xinhai, and C. Lee, "Tunable multiband terahertz metamaterials using a reconfigurable electric split-ring resonator array," *Light Sci. Appl.*, vol. 3, p. e171, May 2014.
- [41] H. Tao, A. C. Strikwerda, K. Fan, W. J. Padilla, X. Zhang, and R. D. Averitt, "MEMS based structurally tunable metamaterials at terahertz frequencies," *J. Infrared Millim. Terahertz Waves*, vol. 32, no. 5, pp. 580–595, 2011.
- [42] H. Tao, W. J. Padilla, X. Zhang, and R. D. Averitt, "Recent progress in electromagnetic metamaterial devices for terahertz applications," *Sel. Top. Quantum Electron. IEEE J.*, vol. 17, no. 1, pp. 92–101, Jan. 2011.
- [43] C. H. Lam, "History of phase change materials," in *Phase Change Materials: Science and Applications*, 1st ed., S. Raoux and M. Wuttig, Eds. New York, NY: Springer, 2009, pp. 1–14.
- [44] A. H. Gwin, "Materials Characterization and Microelectronic Implementation of Metal- Insulator Transition Materials and Phase Change Materials," Air Force Inst Tech, 2015.
- [45] D. Bouyge, A. Crunteanu, J.-C. Orlianges, D. Passerieux, C. Champeaux, A. Catherinot, A. Velez, J. Bonache, F. Martin, and P. Blondy, "Reconfigurable bandpass filter based on split ring resonators and vanadium dioxide (VO<sub>2</sub>) microwave switches," in *Microwave Conference, 2009. APMC 2009. Asia Pacific*, 2009, pp. 2332–2335.
- [46] M. J. Dicken, K. Aydin, I. M. Pryce, L. A. Sweatlock, E. M. Boyd, S. Walavalkar, J. Ma, and H. A. Atwater, "Frequency tunable near-infrared metamaterials based on VO<sub>2</sub> phase transition," *Opt. Express*, vol. 17, no. 20, pp. 18330–18339, Sep. 2009.
- [47] B. Gholipour, J. Zhang, J. Maddock, K. F. Macdonald, D. W. Hewak, and N. I. Zheludev, "All-optical, non-volatile, chalcogenide phase-change meta-switch," in *Lasers and Electro-Optics Europe (CLEO EUROPE/IQEC), 2013 Conference on and International Quantum Electronics Conference*, 2013, p. 1.
- [48] Z. L. Sámson, S.-C. Yen, K. F. MacDonald, K. Knight, S. Li, D. W. Hewak, D.-P. Tsai, and N. I. Zheludev, "Chalcogenide glasses in active plasmonics," *Phys. Stat. Solidi—Rapid Res. Lett.*, vol. 4, no. 10, pp. 274–276, 2010.
- [49] Z. L. Sámson, K. F. MacDonald, F. De Angelis, B. Gholipour, K. Knight, C. C. Huang, E. Di Fabrizio, D. W. Hewak, and N. I. Zheludev, "Metamaterial electro-optic switch of nanoscale thickness," *Appl. Phys. Lett.*, vol. 96, no. 14, 2010.